Synthesis and Vesicle Formation from Dimeric Pseudoglyceryl Lipids with $(CH_2)_m$ Spacers: Pronounced *m*-Value Dependence of Thermal Properties, Vesicle Fusion, and Cholesterol Complexation

Santanu Bhattacharya* and Soma De[a]

Abstract: Eight new dimeric lipids, in which the two Me_2N^+ ion headgroups are separated by a variable number of polymethylene units $[-(CH_2)_m-]$, have been synthesized. The electron micrograph (TEM) and dynamic light scattering (DLS) of their aqueous dispersions confirmed the formation of vesicular-type aggregates. The vesicle sizes and morphologies were found to depend strongly on the *m* value, the method, and thermal history of the vesicle preparation. Information on the thermotropic properties of the resulting vesicles was obtained from microcalorimetry and temperature-dependent fluorescence anisotropy measurements. Interestingly, the T_m values for these vesicles revealed a nonlinear dependence on spacer chain length (*m* value). These vesicles were able to entrap riboflavin. The rates of permeation of the OH^- ion under an imposed transmembrane pH gradient were also found to depend significantly on the *m* value. X-Ray diffraction of the cast films of the lipid dispersions elucidated the nature and the thickness of these membrane organizations, and it was revealed that these lipids organize in three different ways depending on the *m* value. The EPR spin-probe method with the doxylstearic acids 5NS, 12NS, and 16NS, spin-labeled at various positions of stearic acid, was used to establish the chain-flexibility gradient and homogeneity of these bilayer assemblies. The apparent fusogenic propensities of these bipolar tetraether lipids were investigated in the presence of Na_2SO_4 with fluorescence-resonance energy-transfer fusion assay. Small unilamellar vesicles formed from **1** and three representative biscationic lipids were also studied with fluorescence anisotropy and ^1H NMR spectroscopic techniques in the absence and the presence of varying amounts of cholesterol.

Keywords: cholesterol interactions · lipids · membranes · thermotropic properties

Introduction

While the properties of vesicular membranes derived from a large number of *monomeric* natural lipids,[1] such as phosphatidylcholines as well as their synthetic analogues,[2] have been examined in detail, there is very little in the literature that attempts to examine the vesicles prepared from *multimeric* lipids.[3] This is despite the fact that several *multimeric* lipid systems occur naturally and are believed to possess important biological functions. Thus cardiolipins (glycerol-bridged dimeric phosphatidic acid), which constitute a class of complex phospholipids that occur mainly in the heart and skeletal muscles, show high metabolic activity.[4] In addition, association of acidic phospholipids in cell membranes with Ca^{2+} triggers fusion, as Ca^{2+} binding induces formation of dimeric or higher-order lipid complexes.[5] Similarly, glycolipid A, composed of two phosphate headgroups and seven hydrophobic chains, serves as an immunomodulator in the selective recognition of toxins, bacteria, or viruses at the cell surfaces.[6]

Cytomimetic approaches in the design of dimeric and oligomeric amphiphiles[7] that form micelles with unusual morphologies[8] have opened up new vistas in aggregate chemistry. Indeed impressive property modifications are observed from these types of amphiphiles and therefore they are currently receiving a lot of attention.[9] A detailed study of the influence of dimerization on vesicle systems of well-defined synthetic lipids seems to be the most direct approach to understanding the role of these complex amphiphilic molecules in living cells.

We have been interested in the development of new amphiphiles and lipids and in the properties manifested upon their self-organization.[10] Now we turn our attention to synthetic gemini pseudoglyceryl lipids **2**. The presence of an intervening $-(CH_2)_m-$ spacer at the headgroup was found to strongly influence the properties of these lipids at the membrane level. Thus at low and high *m* values ($m = 3$, 4,

[a] Prof. S. Bhattacharya, Dr. S. De
Department of Organic Chemistry
Indian Institute of Science, Bangalore 560 012 (India)
Also at: The Chemical Biology Unit
Jawaharlal Nehru Centre for Advanced Scientific Research
Bangalore 560 012 (India)
Fax: (+91) 80 334-1683
E-mail: sb@orgchem.iisc.ernet.in

  0947-6539/99/0508-2335 $ 17.50+.50/0

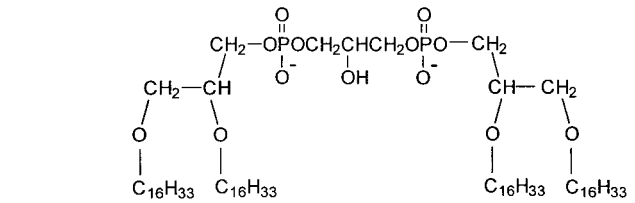

CARDIOLIPIN

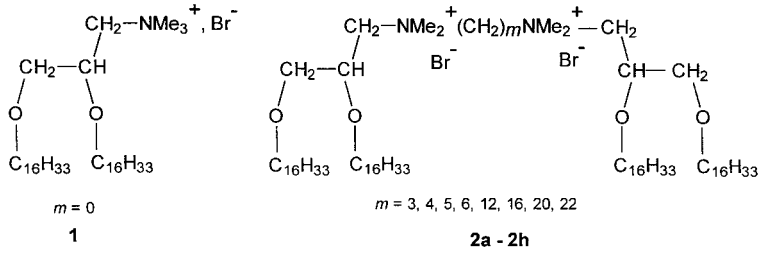

m = 0
1

m = 3, 4, 5, 6, 12, 16, 20, 22
2a - 2h

or 20 – 22), the vesicles are nearly impermeable and show high thermal gel – liquid crystalline transition temperatures. The vesicles formed from lipids with *m* values 5 – 12 show little difference in their melting temperatures, although the transmembrane permeation rates increase with the rise in *m* value. X-Ray diffraction studies on the cast film of these membranes confirm distinct differences in their organization and packing arrangements as a function of *m* value. The evidence of interdigitation of lipids with high *m* values is shown unambiguously from EPR measurements. The intervesicular fusion of membranes derived from dimeric lipids also shows discernible *m*-value dependence. It is also shown that inclusion of even 30 mol % of cholesterol in dimeric lipid membranes does not lead to the abolition of the order – disorder transitions of these membranes.

Results and Discussion

Synthesis: For the synthesis of this new series of biscationic gemini lipids, we considered the pseudoglyceryl backbone as a suitable structural anchor for such lipid construction. This type of building block is ubiquitously present in naturally occurring phospholipids. The structural features of the monomeric analogue of these lipids are similar to that of dioleyloxy-propyl-trimethylammonium chloride (DOTMA) and related derivatives, which are widely used for gene-transfer applications.[11] Long hydrocarbon chains ($nC_{16}H_{33}$) were connected to the glycerol backbone by an ether-type linkage to ensure hydrolytic stabilities of the resulting lipids in both acidic and alkaline conditions even at extreme pH. Dimeric lipids were constructed by covalent insertion of a polymethylene chain through two Me_2N^+ headgroups within a gemini unit, where each unit is composed of 1,2-dihexadecyloxy-propane-3-dimethylammonium ions.[12] In this situation, the distance between the two polar $-NMe_2^+$ groups should be governed by the spacer chain length (*m* value) and its conformation. We also synthesized the corresponding lipid monomer, 1,2-dihexadecyloxypropane-3-trimethylammonium bromide, (**1**) and decided to consider it as the reference *monomeric* lipid ($m = 0$) for the comparison of the vesicular properties of the dimeric lipids. Interestingly, the herein described dimeric lipids, especially with longer spacer chains ($m = 20 – 22$), are also related to the bolaamphiphilic lipids, where the headgroups are linked through the termini of a hydrophobic chain.[13]

We have synthesized altogether eight new *dimeric* lipids **2a – 2h** according to the plan shown in Scheme 1. First the $-CH_2OH$ group of the primary building block, 1,2-isopropylidene glycerol (**3**), was protected in the form of a benzyl ether **4**.

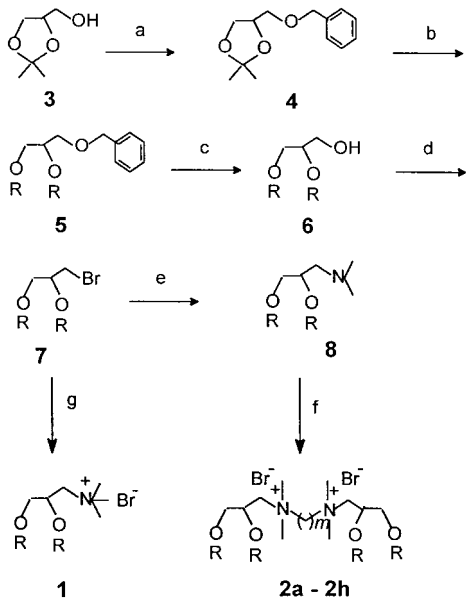

Scheme 1. Conditions: a) $C_6H_5CH_2Cl$, KOH, C_6H_6, reflux, 87 %; b) i) aq. HCl/MeOH, RT 84 %; ii) $nC_{16}H_{33}Br$, KOH, C_6H_6, reflux, 58 %; c) Pd-C/H_2, 93 %; d) CBr_4, PPh_3, CH_2Cl_2, 90 %; e) Me_2NH/EtOH, heat, pressure tube, 95 %; f) $Br(CH_2)_mBr$, reflux, 60 – 75 % (exact yields depend on *m*); g) Me_3N/EtOH, heat, pressure tube, 90 %.

The isopropylidene group from **4** was then removed by treatment with HCl in aqueous MeOH, and the diol obtained upon preparative chromatography over silica gel was dialkylated with 2.2 equivalents of $nC_{16}H_{33}Br$ to give **5** (58 % yield). Upon hydrogenolysis of **5**, compound **6** was formed in ≈93 % yield. In the subsequent step, **6** was converted to the corresponding bromide **7** in a ≈90 % yield by reaction with PPh_3/CBr_4 in dry CH_2Cl_2. Compound **7** was quaternized in the presence of Me_3N in EtOH to give **1** in ≈80 % yield. The bisquaternary lipids **2a – 2h** were obtained from the corresponding dimethylamino derivative, **8** upon refluxing with individual alkanediyl-α,ω-dibromides in 60 – 75 % yields. All the compounds gave expected analytical and spectroscopic

0947-6539/99/0508-2336 $ 17.50+.50/0 *Chem. Eur. J.* **1999**, *5*, No. 8

data consistent with their molecular structures, see the Experimental section.

Vesicle formation and characterization: We first examined the vesicle-forming abilities of the above lipids in water. Reversed-phase evaporation (REV) and sonication methods have been used to obtain large and small vesicles, respectively. All the dimeric lipid vesicles prepared by either protocol remained stable for several days, except the one with $m = 3$. The size and nature of the vesicle were found to depend strongly on the lipid concentration, thermal history, and the method of vesicle preparation. Thus while vortexing afforded mainly open lamellae and sonication gave small, spherical, closed microstructures, REV gave predominantly multilamellar, spherical vesicles (MLVs). Because of larger sizes, we decided to closely examine the transmission electron microscopy (TEM) of the MLVs prepared from these lipids generated by REV.

TEM examination of the individual, air-dried, opalescent aqueous suspensions of **2a**–**2h** layered on carbon/formvar-coated copper grids revealed the existence of *closed,* multilamellar aggregates in all the cases. The average diameters of **2a**, **2d**, **2e**, and **2h** were 290 ± 20 Å, 740 ± 25 Å, 880 ± 50 Å, and 1500 ± 25 Å, respectively. Closer scrutiny of the micrographs also revealed that lamellar widths of each lipid aggregate were in reasonable accord with the results extrapolated from the XRD measurements (see below).

Dynamic light scattering (DLS): Lipid dispersions of **1**, **2a**–**2h** obtained by bath sonication of the hydrated lipid film followed by three freeze–thaw cycles afforded vesicles with virtually unimodal distribution of particle diameters as revealed by DLS (Table 1). Examination of DLS data shows that vesicles from dimeric lipids were invariably larger than their monomeric counterpart ($m = 0$). However, the variation of the hydrodynamic diameter as a function of m value was found to be quite complex. Hence, the vesicular size was found to be the largest for lipid **2** with $m = 3$, then decreased with an increase in m value up to $m = 12$, and again increased with $m > 12$. These sizes were also found to be in agreement with the TEM data on sonicated vesicles.

Table 1. Riboflavin entrapment and apparent OH^- permeation rates across different bilayer membranes at 25 °C.[a]

	Lipid conc. [mM]	Hydrodynamic diameter [nm][b]	% entrapment [c]	$t_{1/2}$ [min]	$10^3 k_{perm}$ [s^{-1}]	$10^8 P$[d,e] [$cm\,s^{-1}$]
2a	0.73	93	2.16	[f]	–	–
2b	0.72	52	2.13	21.9	0.5	0.72
2c	0.71	29	4.13	10.2	1.1	0.47
2d	0.71	29	1.87	4.9	2.4	0.99
2e	0.67	30	1.61	1.9	6.2	4.56
2f	0.63	37	2.02	0.7	15.6	17.1
2g	0.62	50	2.18	[g]	–	–

[a] The time-dependent decay of fluorescence intensity at ~514 nm was monitored as a function of time. In each case, the extent of decay was followed beyond 90%. The decay followed an apparent monoexponential path. The rate constant values represent averages of three independent experiments, and the reproducibility was ±3% for individual samples. [b] As obtained from DLS. [c] The entrapment of riboflavin given in percentages has been corrected for an apparent absorption of marker molecules in each case. [d] P is the permeation constant of OH^- toward vesicles at pH 10.2. [e] Diameters of the vesicles and bilayer thicknesses were obtained from DLS measurements and XRD studies, respectively. Time-dependent loss of fluorescence intensity may be interpreted as a permeation-limited deprotonation of riboflavin entrapped in the internal aqueous compartment by OH^-. [f] No significant time-dependent changes in fluorescence was seen at 25 °C. However, upon heating the vesicle beyond T_m resulted in the release of the doped dye. [g] The decay is instantaneous.

Dye entrapment: In order to examine the entrapment abilities, vesicles from **2a**–**2g** (1 $mg\,mL^{-1}$) were generated by dispersal in a bath sonicator over a period of ≈30 min at ≈70 °C in water (pH 5.8) containing riboflavin (2×10^{-5} M). Gel-filtration chromatography with a sephadex G-50 column was performed to separate riboflavin-entrapped vesicles from the free, unbound riboflavin. As previously observed[14] some riboflavin molecules adhered to the aggregate interfaces, while a few got entrapped inside the vesicles. Importantly, however, in all the cases, riboflavin-associated vesicles could be separated from the free riboflavin dye. Relevant data on the percentage entrapment of riboflavin for various lipids are given in Table 1.

Transmembrane permeation: Riboflavin is fluorescent in its neutral form and upon deprotonation ($pK_a \approx 10.2$) it loses its fluorescence. The emission due to the membrane-associated total riboflavin was measured at 514 nm upon excitation at 374 nm at 25 °C. At this temperature all the vesicular aggregates remained in their rigid gel-like states (see below). As the pH of the vesicular solution was raised from 5.8 to 10.2, the fluorescence intensity (514 nm) decreased initially instantaneously to about 63 ± 3% for **2a**, 83 ± 4% for **2b** and **2c**, and 72 ± 4% for **2d**–**2g** of the original value (recorded prior to pH adjustment). We attribute this instantaneous loss in the fluorescence intensity to the deprotonation of the riboflavin molecules that were bound at the exovesicular surfaces. However, the residual fluorescence intensity disappeared as a function of time for the vesicular solutions of **2b**–**2f**, but remained virtually unchanged for **2a** and **2g**. Since the residual losses in the fluorescence intensities followed monophasic time dependence for **2b**–**2f**, numerical fitting of the kinetic data could be achieved by means of the monoexponential relation. The half-times of this process ($t_{1/2}$) for all of these vesicles and the related data are given in Table 1.

Using the respective bilayer thicknesses as obtained from XRD studies (see below) and assuming the time-dependent loss of riboflavin fluorescence as a rate-limiting permeation of exovesicular OH^- into the vesicle's interior aqueous compartment, we can calculate the permeation constant (P in $cm\,s^{-1}$) of OH^- towards vesicles at pH 10.2. The differences in OH^- permeability provide useful information about the vesicular packing. The rate of permeation or permeability constant of the individual vesicular system clearly appears to depend significantly on the length of the spacer chain (m value) connecting the two NMe_2^+ groups. Thus changing the m value from 4 to 16 leads to >31-fold increase in the transmembrane permeation rates. When corrected for bilayer thicknesses the corresponding ratio remains at >24. With the increase in spacer chain length ($m \geq 3$), the rate of OH^- permeation increases, presumably because of the increased spacer chain

looping and consequent loss of tightness in the molecular packing.

Interestingly, with vesicular **2a** and **2g** the initial fluorescence intensity underwent a rapid decay upon pH adjustment (5.8 →10.2). However, subsequent time-dependent losses of fluorescence were not recorded with vesicular **2a** and **2g** at 25 °C as was observed with the vesicles of **2b**–**2f**. We believe that the observed resistance to transmembrane permeation with the vesicular **2a** may originate from the tight nature of the lipid packing in these bilayers at 25 °C (gel state). Indeed when the riboflavin-loaded vesicles of **2a** were heated above their T_m, time-dependent monophasic fluorescence decay could be clearly seen. Interestingly, the corresponding plot of the fluorescence emission (after pH adjustment) against T broke at a temperature that was comparable with the corresponding T_m value for the vesicular systems of **2a**. In the case of the corresponding gel-filtered vesicles of **2g**, however, thawing beyond T_m did not show any evidence of riboflavin release. It appears that the decay of the emission intensity from **2g** is so fast at 25 °C that it merges with the initial instantaneous decrease in fluorescence. This in turn indicates that the lipid packing in vesicular **2g** is quite loose making it very leaky under the experimental conditions described.

Thermotropic phase-transition behavior: A well-defined, sharp, single, main phase transition (gel →liquid crystalline) peak (T_m) was observed from practically all the dispersions during the heating runs in DSC. In addition to a peak due to the main transition for **2a**, two minor peaks at ≈66 and 71 °C were also observed. Suspensions of each of **1**, **2a**, **2b**, and **2c** also showed one clearly detectable peak due to pre-transition, which appeared at approximately 10 °C, prior to the main transition. All lipid suspensions showed virtually reversible transition behavior during heating as well as cooling runs. At different scanning rates, identical values of enthalpy, T_m, and the height of the transition profile were obtained.

Thermotropic properties of vesicular **1** and **2a**–**2h** at much lower concentrations (1.0–2.5 mM) were also examined by microcalorimetry. Vesicular specimens of the lipids with $m =$ 0, 3, 4, and 5 reproduced the main T_m values observed at 115 mM, and also showed the presence of distinct pre-transition peaks, a phenomenon often observed with the melting of natural phospholipids. Additional minor peaks at 66.1 and 71.6 °C for **2a** and 58.0 °C for **2g** were also observed. HPLC analyses of the DSC samples of either **2a** or **2g** confirmed that additional peaks were not due to the presence of any impurities or caused by lipid decomposition.

Since DSC and microcalorimetry results at high and low lipid concentrations, respectively, were essentially the same, we have confined our discussions to microcalorimetry only. The solid-to-fluid melting transition temperatures (T_m) of various members of **2** depend strongly on the m value of the spacer chain [$-(CH_2)_m-$]. Relative to **1** ($m = 0$), there is a substantial increase in the T_m values of the membranes derived from dimeric **2a**. In addition, unlike the membranes that are assembled from **1**, which show a sharp endothermic main transition at ≈45 °C, those made from **2a** exhibit a more complex melting pattern. Upon dispersion in water, the hydrocarbon chains in **1** tend to avoid water exposure and thus self-aggregate. Although its chains pack closer, the cationic Me_3N^+ headgroups tend to stay away from each other within the vesicles to avoid unfavorable electrostatic repulsion. Thus in the bilayers, an equilibrium distance between the Me_3N^+ groups in **1** is maintained as a result of compromise between the two opposing tendencies. However, in dimeric lipid **2** with $m \leq 4$, the distance between the Me_2N^+ groups within a gemini unit is shorter than the equilibrium separation between the monomeric Me_3N^+ groups in vesicular **1**. This is true even when the spacer chain in **2a** or **2b** adopts a fully extended s-*trans* conformation. An obvious consequence of this is the more efficient packing within vesicular **2a** or **2b** compared with **1**. As the headgroup separation in **2** approaches the equilibrium distance with the increase in m value, the packing organization in the dimeric lipids start to simulate that found in **1**. The observed variations in the vesicular properties as a function of their spacer chain lengths with the herein described dimeric lipids are analogous to those of the micelle-forming gemini amphiphiles described by Zana.[15] Hence, the solid-to-fluid transition temperatures of **2c**–**2e** ($m = 5$, 6, 12) are quite similar to that of vesicular **1**. On the other hand, the melting transition profiles of the dimeric lipids, $m \geq 16$, appeared to be considerably broader (hence less cooperative) than their counterparts with $m \leq 12$, whose melting transitions were quite sharp. The increased propensity of the spacer chain looping in $m = 6-16$ might impair the interlipid packing in these vesicles and lead to lower melting temperatures than that of **2a** or **2b**. The melting profiles for lipids with $m = 20-22$ were, however, broader although their T_m values were quite high. This suggests that the membrane organizations and packing motifs of gemini-lipid units with high m value (≥ 16) are quite different from that of the lipids with low and intermediate m values. The T_m values and cooperativity units (CU) are compared as a function of m value in Figure 1.

In general, the ΔH and ΔS values for the main transition of lipids with varying m values are linearly correlated with T_m values except for **2a** ($m = 3$). The presence of multiple transitions makes the situation complex for **2a**. However, when the enthalpic contributions of other transitions are added to that of the main transition, one finds reasonable correspondence for the total ΔH_{calcd} value with the entire melting transition of **2a**. It should be noted that dimers **2a**–**2h** are mixtures of two diastereoisomers. Therefore the complex melting behavior manifested with **2a** may originate from the formation of small phase-separated domains of the different diastereomeric components. It is possible that such phase segregation may be significant only when the spacer chain length is small ($m = 3$), and with higher m values the corresponding lipid diastereomers could somehow accommodate each other and mix well giving rise to a single T_m value.

Fluorescence anisotropy measurements: All the lipid dispersions showed reasonably cooperative main phase transitions (T_m) in the plots of r versus T (Figure 2). The breaks related to the T_m from these plots were generally similar to the T_m values obtained from microcalorimetry, except for the lipids with $m = 20$ and 22, which showed broader and apparently lower

0947-6539/99/0508-2338 $ 17.50+.50/0 *Chem. Eur. J.* **1999**, *5*, No. 8

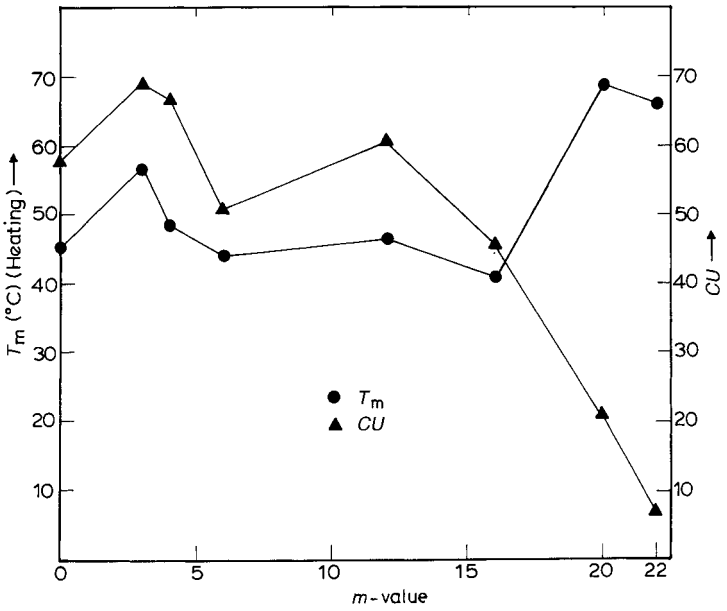

Figure 1. Dependence of thermotropic phase-transition temperature (T_m) and cooperativity unit (*CU*) of different amphiphiles **1**, **2a**–**2h** on *m* values.

T_m values (≈62 and ≈58 °C, respectively) in this experiment. The observed broadness in the *r* versus *T* transition profiles are consistent with lower *CU* values seen in calorimetric studies. The apparent orders of the lipid hydrocarbon chains at both above and below T_m were also found to be influenced by their *m* values. Figure 2 (inset) shows the variations of *r* values above and below T_m with *m* value. Thus with the

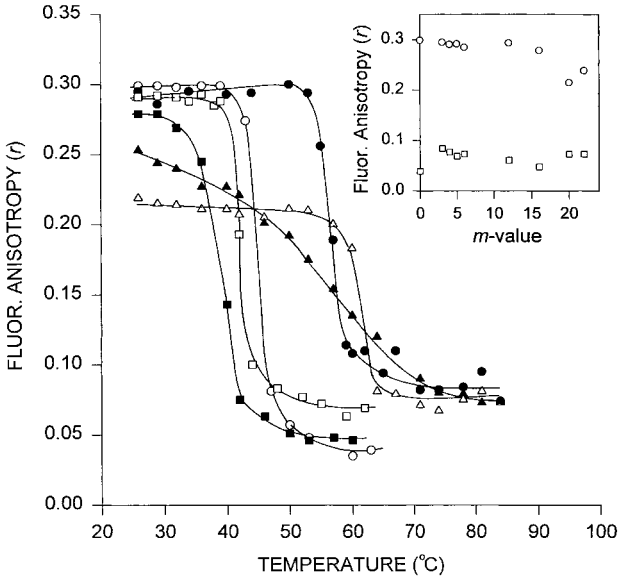

Figure 2. Fluorescence anisotropy (*r*) versus *T* [°C] plots for vesicular **1** (○), **2a** (●), **2c** (□), **2f** (■), **2g** (△), and **2h** (▲) samples. The inset shows the variations of *r* values with *m* value at above (□) and below (○) T_m.

increase in *m* value (≥16), the apparent order in the gel state of these bilayers was found to be considerably less than their low *m* value counterparts. At the same time the lipids with *m* = 3, 4, and 20–22 became less fluid above T_m relative to their intermediate *m* value counterparts. This could be a consequence of perturbation within the Me_2N^+ headgroups and/or direct interaction of the spacer chain with the nonpolar hydrocarbon chain segments. Taken together these results point towards the differences in organizational features of the membranes with lipids of *m* > 16 to their low *m* value counterparts.

X-Ray diffraction (XRD): In order to gain information on the lamellar thicknesses of these aggregates, self-supporting cast films of aqueous dispersions (10 mg mL^{-1}) of **1** and **2a**–**2h** were examined by X-ray diffraction. A series of higher order reflections for all the lipid dispersions were observed in the diffraction patterns. Table 2 summarizes the long spacings obtained from the cast films of each of these lipids, and these results clearly suggest the formation of different kinds of aggregates from lipids of various *m* values.

Table 2. Unit layer thicknesses obtained from XRD studies of self-supporting cast films of **1**, **2a**–**2h** and their proposed packing.

Lipid *m* value	Unit bilayer thickness [Å] observed[a]	calculated[b]	Proposed packing[c]
0	49.58	49	C_{16} bilayer
3	48.07	49	C_{16} bilayer
4	49.81	49	C_{16} bilayer
5	49.12	49	C_{16} bilayer
6	49.35	49	C_{16} bilayer
12	31.95	49, 16.8,[d] 31[e]	Tilted interdigitated bilayer
16	29.59	9, 21.9,[d] 31[e]	Tilted interdigitated bilayer
20	29.80	49, 27[d]	Monolayer–bilayer
22	30.30	49, 29[d]	Monolayer–bilayer

[a] As obtained from reflection XRD of cast films. [b] Lengths of two molecular layers of lipids as obtained from energy-minimized CPK models (INSIGHT). [c] See Figure 6. [d] Length of unit monolayer–bilayer arrangment of lipids as obtained from energy-minimized CPK models. [e] Length of unit tilted, interdigitated bilayer arrangment of lipids as obtained from energy-minimized CPK models.

The diffraction patterns of **1** and **2a**–**2d** showed membrane thicknesses (*d*) of 49.6, 48.1, 49.8, 49.1, and 49.3 Å, respectively, on the basis of the higher order reflections (*n* = 3, 4, 5, 6). Assuming the long hydrocarbon chains in these lipids to be primarily in an s-*trans* conformation, the widths of these bilayers were estimated to be ≈49 ± 1 Å from the CPK model of the two molecules oriented parallel to the bilayer normal (see below). This suggests the formation of a *untilted* bilayer arrangement (Figure 3a) with lipid **1** and the gemini lipids of *m* values 3, 4, 5, and 6. These cast films, however, did not show any evidence of polymorphism as other types of reflections were not observed. Cast films of dispersions of **2e** (*m* = 12)

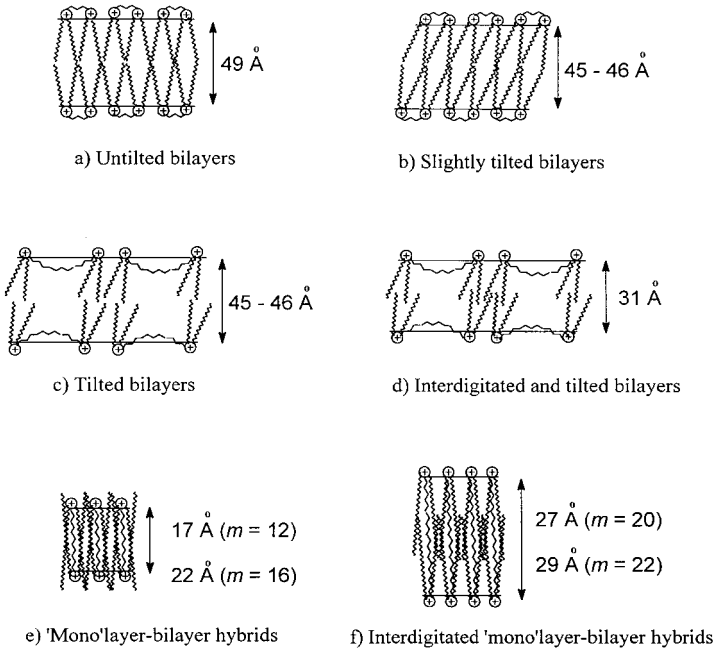

Figure 3. Schematic representation of possible bilayer forming motifs with *gemini* lipids as a function of *m* value.

and **2f** ($m = 16$) were found to consist of considerably thinner intercalated layers with thicknesses of 32 and 29.6 Å, respectively. Such widths of unit layers cannot be explained by tilting alone (Figure 3c). Probably these lipid molecules interdigitate at the midplane of the bilayers in addition to tilting with respect to the bilayer normal (Figure 3d). Since the spacer chain is quite long for these lipids, looping is increasingly favored. So, the propensities of these additional modes of lipid packing increase, this also helps to fill the voids that might otherwise be created inside the lipid assemblies. An alternative mode shown in Figure 3e is not feasible, as in this situation the hydrocarbon chains have to protrude into the polar headgroup regions.

Cast films of dispersions of **2g** and **2h** exhibited one series of higher order reflections corresponding to layer thicknesses of 29.8 and 30.3 Å, respectively. These values compare favorably with the stacked lamellae thickness of ≈28 Å found for another model archaebacterial membrane lipid developed by Thompson et al.[13e] To explain their reflection XRD data, we suggest a kind of monolayer–bilayer hybrid organization as shown in Figure 3f. Since these lipids exhibit high T_m values, the possibility of formation of interdigitated, tilted, bilayers (Figure 3d) may be ruled out.

EPR spectra in the gel phase: The EPR technique has been frequently used to understand the nature of phases, for example, mixed or fully interdigitated, that occur in the gel phase.[16] Here, we have investigated the hydrocarbon chain packing in conjunction with the possible effects of spacer chain looping using a series of fatty acid spin labels with the nitroxide group located at specific positions along the chain in the gel state. This study is based on the relative changes in rotational motion and order parameters of the fatty acid spin labels embedded in the vesicular dispersions.

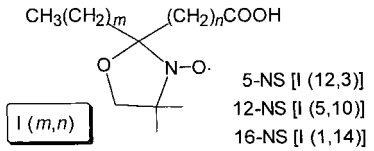

The first harmonic absorption EPR spectra of different fatty acid spin-label positional isomers incorporated in vesicular dispersions are shown in Figure 4. At 25 °C, the spectra for **1**, **2a**, and **2e** display a lesser degree of immobilization on proceeding towards the terminal methyl end of the chain from the polar headgroup region as they exhibit extensive motional narrowing of the hyperfine aniso-

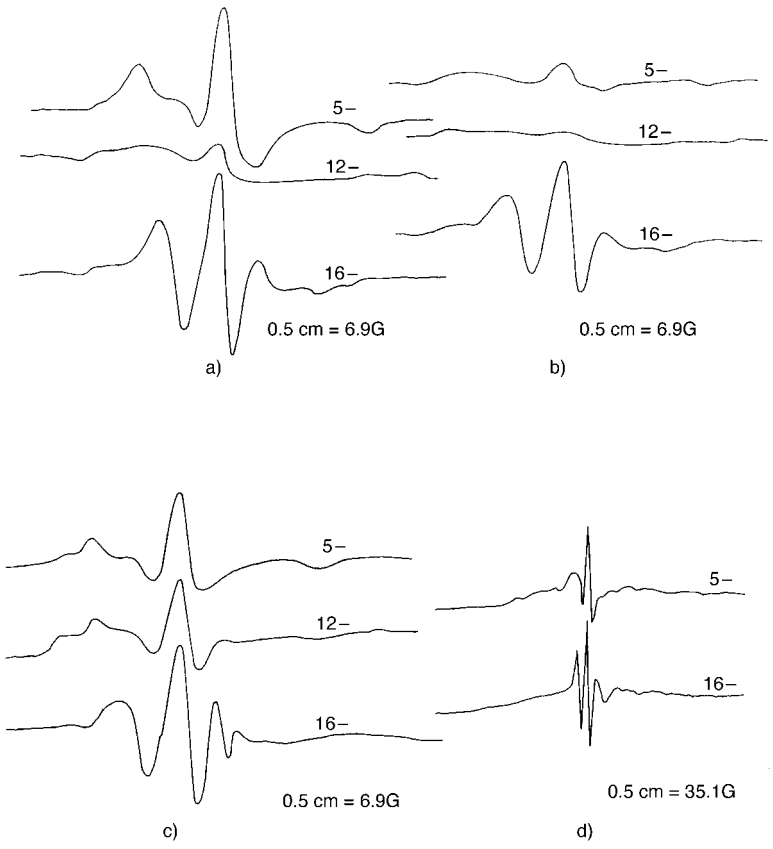

Figure 4. EPR spectra of 5-, 12-, and 16-doxylstearic acids at 25 °C incorporated in solid gel phases of membranes of a) **1**, b) **2a**, c) **2e**, and d) **2g**.

0947-6539/99/0508-2340 $ 17.50+.50/0 *Chem. Eur. J.* **1999**, *5*, No. 8

tropy on the conventional EPR time scale. However, there is a substantial difference in the chain mobility as a function of lipid *m* value. For lipids with $m=0$ (**1**) and 3 (**2a**), the *immobilization* of the hydrophobic tail appears to increase from position-5 to position-12, thereafter it decreases again at position-16. This is obvious when one compares both the splittings and the widths of the outer hyperfine lines ($T_{\parallel}$) of the spectra (Figures 4 and 5, Table 3). The $T_{\parallel}$ value

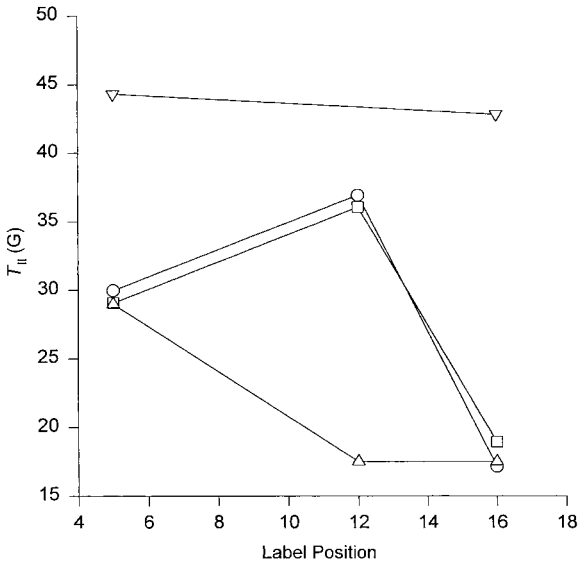

Figure 5. Outer hyperfine splitting $T_{\parallel}$ (G) as a function of the label position, in the fatty acid spin labels in dispersions of **1** (○), **2a** (□), **2e** (△), and **2g** (▽).

Table 3. ESR spectral parameters of fatty acid spin labels in **1**, and **2a**–**2h** at 25 °C.[a]

	Fatty acid spin label	$T_{\parallel}$ [G]	$\tau_0 \times 10^{-9}$ [s]	*S*
1	5-NS	29.98	21.17	0.454
	12-NS	36.92	–	–
	16-NS	17.16	3.53	0.297
2a	5-NS	29.07	10.4	0.524
	12-NS	36.05	–	–
	16-NS	18.94	5.4	0.363
2e	5-NS	28.98	10.07	0.463
	12-NS	17.51	10.27	0.335
	16-NS	17.51	1.78	0.326
2g	5-NS	44.31	8.44	0.556
	16-NS	42.82	2.23	1.0

[a] See Experimental Section for the details.

(≈30 G) obtained for these bilayers is in good agreement with that of 1,2-dipalmmitoyl-*sn*-glycero-3-phosphocholine (DPPC; ≈30.8 G) in HEPES buffer (pH 7.4) as sensed by 5-NS, incorporated in the vesicular DPPC.[16b] It is to be noted that for **2e** ($m=12$), there is little difference in spectral anisotropy with the label at the 12-position compared with that at the terminal methyl end.

In contrast, the maximum hyperfine splittings, $T_{\parallel}$, of the spectrum of a fatty acid, spin-labeled near the chain terminal, 16-NS for **2g** ($m=20$) are significantly larger compared with those for **1**, **2a**, and **2e**. Strikingly, this value remains almost unchanged when one compares this with that of a segment labeled much closer to the polar headgroup region (5-NS). This is because the terminal methyls of the fatty acid chains of lipids in **2g** are located near the bilayer-aqueous interface, presumably owing to the formation of a interdigitated monolayer–bilayer kind of lipid organization. This type of behavior is reported in the literature[17] for the interdigitated lipid phases in phosphatidylcholine (PC) and phosphatidylglycerol (PG) induced by glycerol and polymyxin, respectively. Hence these results can be attributed to the formation of fully interdigitated lipid bilayers by **2g** compared with the noninterdigitated gel-phase lipid bilayers by **1**, **2a**, and **2e**. These results and conclusions are in accord with the results obtained from the other studies.

Fusion assay: Since the primary function of membranes is to maintain the integrity of cells within their environment and to maintain the organization of subcellular compartments inside the cell membrane, events like fusion have to be adequately regulated in space and time. Information about the tendencies of **1** and **2a**–**2h** to fuse under given conditions is useful, since the molecular packing in the membranes is delicately balanced depending on the *m* value of the lipid dimers. We also wanted to know whether a temporal separation of the membrane leaflets of the interacting vesicles would be allowed with these dimeric lipids. This is important, since the formation of a hemifusion intermediate requires a temporal separation. These considerations prompted us to explore the relative fusion efficiencies of individual vesicular systems, especially those composed of membrane-spanning lipids. Here we present the relative fusogenic properties of vesicular **1**, **2b**, **2d**, **2e**, and **2g** induced by the inorganic anion SO_4^{2-}.

In this study we employed the fluorescence resonance energy transfer (FRET) assay[18] that relies upon the overlap between the emission and excitation spectrum of two, nonexchangeable, fluorophoric phospholipid analogues, *N*-NBD-PE (donor) and *N*-Rh-PE (acceptor). Since the efficiency of FRET between the two given fluorophores is dependent upon their spatial separation, this technique provides the details of how lipid mixing occurs during membrane fusion. The fluorophores have been incorporated into dimeric lipid membranes at concentrations that do not

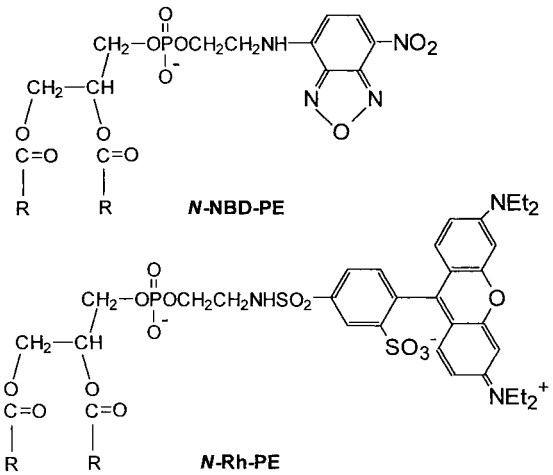

perturb the parent membrane structure. In this situation the efficiency of energy transfer should be proportionally related to their surface density. Upon fusion of fluorescently labeled vesicles with nonlabeled vesicles (probe dilution method),[19] bilayer mixing reduces the surface density of the fluorophores and results in a decrease of FRET efficiency; this can be followed continuously either as an increase in donor NBD fluorescence or a decrease in the fluorescence of the acceptor rhodamine.[20]

When cationic vesicles containing both *N*-NBD-PE (0.6 mol%) and *N*-Rh-PE (0.6 mol%) were incubated with an equal amount of nonlabeled vesicles, no change in the rhodamine fluorescence could be detected. This indicates that the probes did not spontaneously transfer by means of a mechanism with the involvement of diffusion of monomers through the aqueous phase between labeled and nonlabeled membranes. In the presence of Na_2SO_4 (10 mM), however, a slow decrease in the rhodamine fluorescence was observed (Figure 6) in all the cases, except that with **2g**. This suggests

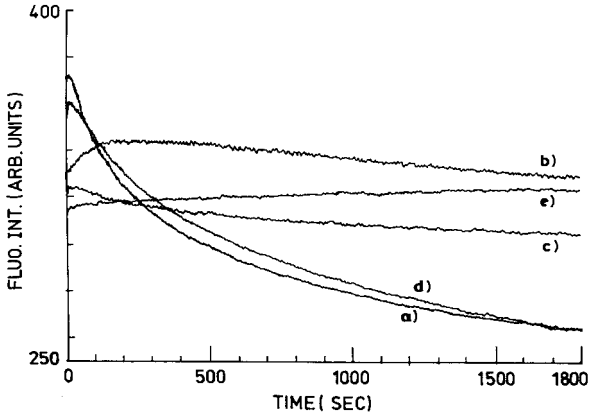

Figure 6. Decay of rhodamine fluorescence with time: a) **1**, b) **2b**, c) **2d**, d) **2e** and e) **2g**.

that Na_2SO_4 probably induces fusion and intermixing of membrane lipids among the liposomes of **1**, **2b**, **2d**, and **2e**. Importantly, however, the rate of this fluorescence decay is different for membranes with different *m* values. For comparison, the percentage change in fluorescence (% $\Delta F/\Delta F_{min}$) for each lipid vesicle was plotted against time (Figure 7). While the percentage change in fluorescence for **1** was 60.7% after 30 min, for **2b** it was only 5.6% after the same period. This is probably because of the rigidness of the bilayer packing in the case of **2b** ($m = 4$) compared with that of monomeric **1** ($m = 0$). However, the percentage change in fluorescence intensity was enhanced with the increase in spacer chain length up to a certain *m* value (17.0% for **2d** and 56.7% for **2e** after 30 min of the injection of salt solution to the vesicular dispersions). This could indicate possible fusion of these membranes through a process that involves transient separation of two bilayer leaflets and the formation of a hemifusion intermediate structure.

In contrast, the vesicles of **2g** showed no decrease in the rhodamine-fluorescence intensity with time. Instead it showed a marginal increase in the fluorescence intensity. It is not apparent why this happens. One possibility is that this may be

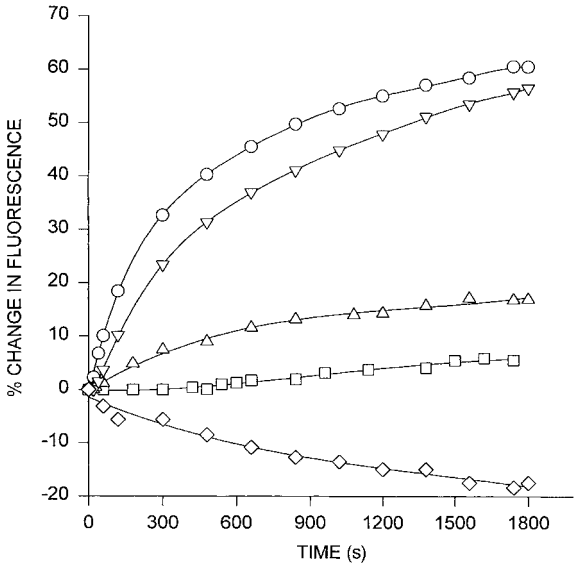

Figure 7. Percentage change in fluorescence with time, **1** (○), **2b** (□), **2d** (△), **2e** (▽) and **2g** (◇).

a result of the onset of aggregation between the vesicles of **2g**, and this is *generally* not observed in the probe dilution method.[19] Very little is known about the fusogenic properties of bolaform lipids. It may be possible that larger energy barriers and greater geometrical constraints are involved in the fusion of membranes composed of this lipid ($m = 20$); these resemble membranes formed from bolaamphiphiles. Indeed a similar phenomenon is reported for the lipids extracted from the thermophilic archaeon *Sulfolobous solfataricus* irrespective of the fusogen employed,[20] while the large unilamellar liposomes composed of bipolar tetraether lipids extracted from the thermophilic archaeon *Sulfolobous acidocaldarius* were found to undergo a nonleaky fusion process in the presence of calcium phosphate, the rate being dependent on the pH and the concentration of the salt.[21]

Interaction of dimeric lipids with cholesterol: Cholesterol is an integral part of mammalian-cell membranes[22] and it is known to noncovalently associate with different lipids within the cell.[23] Such interactions lead to an increase in the orientational order of lipid hydrophobic chains in membranes.[24] This in turn abolishes the solid→fluid transition temperature of the resulting bilayers.[25] Does cholesterol interact with dimeric lipids in the same way as it does with monomeric lipids? Are such interactions dependent on the *m* value of the lipid dimers? To examine the effects of cholesterol inclusion in dimeric lipid membranes, we have employed two widely used methods, that is, fluorescence anisotropy and ^1H NMR spectroscopy.

We measured the fluorescence anisotropy (*r*) of 1,6-diphenyl-1,3,5-hexatriene (DPH) solubilized in different vesicular assemblies in the presence or absence of cholesterol. For this study we selected four representative lipids **1** ($m = 0$), **2a** ($m = 3$), **2e** ($m = 12$), and **2g** ($m = 20$), which were shown to form three different types of membrane organizations. Figure 8 (a–d) shows that the effect of cholesterol incorporation on the thermal behavior of a given lipid depends on the

0947-6539/99/0508-2342 $ 17.50+.50/0 *Chem. Eur. J.* **1999**, *5*, No. 8

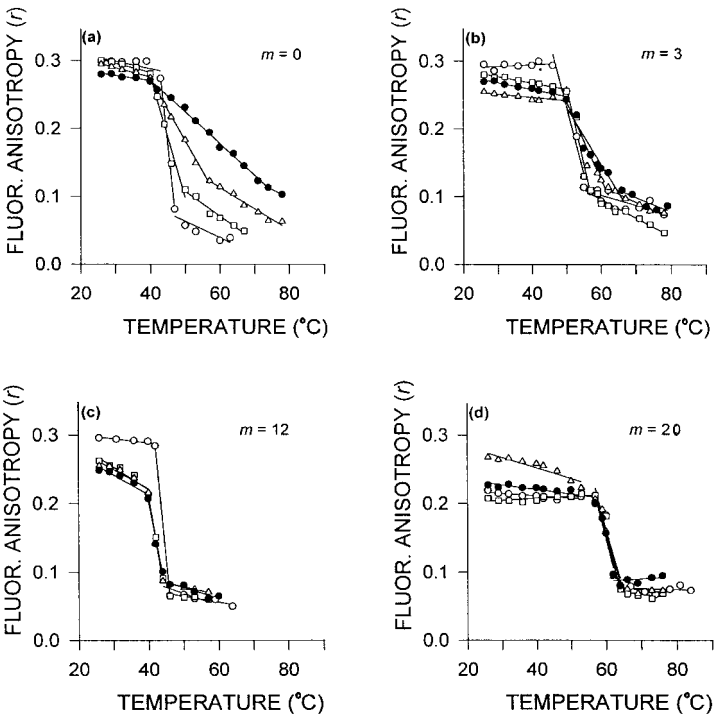

Figure 8. Fluorescence anisotropy (r) versus temperature plots for lipid vesicles: a) **1**, b) **2a**, c) **2e** and d) **2g** with 0 mol% (○), 10 mol% (□), 20 mol% (△) and 30 mol% (●) cholesterol.

lipid structure, in particular on the m value. With vesicular **1**, the breaks in the r versus T plot signifying the melting transition became gradually blurred with the increase in cholesterol percentage. This type of behavior is reminiscent of that reported for cholesterol-phosphatidylcholine[26] and cholesterol–cationic-lipid[10f] mixtures. While the order in the gel phase was little influenced by the inclusion of cholesterol in **1**, it was substantially enhanced in its fluid state. In contrast, breaks related to solid→fluid melting were not abolished even after inclusion of 30 mol% cholesterol in the case of the dimeric lipids. Remarkably, with dimeric lipids upon cholesterol incorporation, the orders in their fluid states were hardly affected, while the resulting mixtures in their gel phases were rendered disordered. We believe that the presence of a $(CH_2)_m$-spacer chain in these lipids influences the location of cholesterol in the resulting membranes, and it is the temperature-induced conformational variation of the spacer chain that predominantly regulates the solid→fluid transition even when cholesterol is present.

To further ascertain the nature of the dimeric-lipid–cholesterol interactions in their fluid states, various cholesterol-free and cholesterol-laced vesicular preparations were analyzed by ^{1}H NMR spectroscopy above their T_ms. Studies were carried out at 60 °C for **1**, 65 °C for **2a**, and 70 °C for **2g**. Compound **2e** was not studied by this method, since the order in its fluid state remained almost unaffected upon incorporation of cholesterol as observed from its r versus T plot. Figure 9 shows the ^{1}H NMR spectra of chain polymethylene $(CH_2)_n$ and terminal methyl groups (CH_3) for different lipid systems in the absence and presence of cholesterol. Addition of cholesterol in increments (0–30 mol%) led to progressive broadening of the downfield $(CH_2)_n$ proton signals in **1**, indicating that inclusion of cholesterol significantly restricted the mobility of the $(CH_2)_n$ units; however, it had much less effect on the terminal CH_3 groups. Similar results were also reported for cholesterol doped phosphatidylcholine vesicles.[23b, 26] Strikingly, the virtually opposite observation was recorded with **2a**. Both the resonances due to $(CH_2)_n$ and CH_3 got sharpened with the increasing percentage of cholesterol. Under comparable conditions **2g**, however, showed a complex behavior. Addition of cholesterol (10 mol%) initially broadened both the $(CH_2)_n$ and terminal CH_3 signals. With 20 mol% cholesterol, these signals became considerably sharper. However, with 30 mol% of cholesterol these signals appeared to broaden again.

The observed differences in the interactions of cholesterol with different types of cationic lipids could be explained on

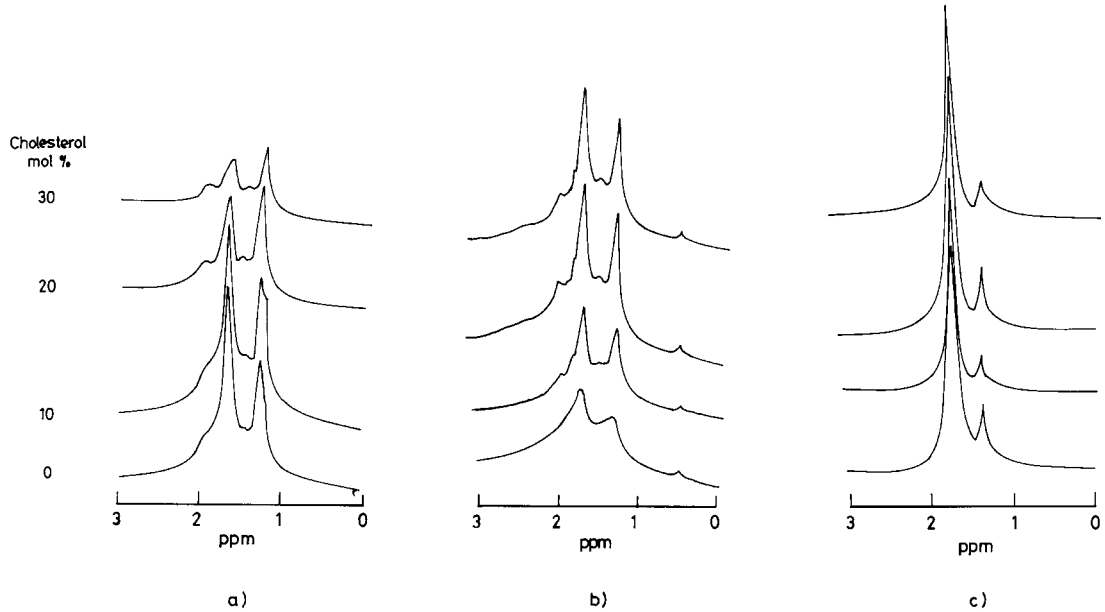

Figure 9. The ^{1}H NMR spectra of chain polymethylene $(CH_2)_n$ and terminal methyl (CH_3) groups for different lipid systems in the absence and presence of different mol% of cholesterol above T_m, a) **1** (at 60 °C), b) **2a** (at 65 °C), and c) **2g** (at 70 °C).

the basis of variations in the molecular packing of these lipids in the vesicular matrices. The interaction between **1** and cholesterol should originate mainly from the hydrophobic contacts, unlike lipids containing ester or amide groups in which hydrogen bonding takes place between the lipid monomer and 3β-OH of cholesterol in addition to the hydrophobic interactions. Thus **1** should be able to accommodate cholesterol in the membrane depending on the miscibility of the latter. Since it is believed that above the T_m value of the lipid, the presence of cholesterol induces additional phases;[27] membrane fluidity also changes accordingly. Current findings indicate that, in general, the membranes composed of dimeric lipids can withstand insertion of more cholesterol compared with the monomeric counterparts. This is a significant observation. Generally inclusion of cholesterol stiffens the resulting membranes. It appears that since the herein described lipid dimers have four hydrocarbon chains, the cholesterol inclusion into such membranes does not lead to a significant increase in the orientational order of the resulting aggregates.

Conclusion

The series of experiments described above, reveal the effects of lipid dimerization. The introduction of a polymethylene spacer chain at the headgroup brings about a dramatic effect on the aggregation behavior, membrane organization, and lipid packing. Dimeric lipids with low *m* values (3, 4) and high *m* values (20–22) showed exceptional thermal, lipid-packing, and cholesterol-association properties. Possibly because of an increase in headgroup bulk and spacer chain looping with the rise in *m* value up to $m \leq 16$, the membranes from the corresponding lipids show a poor hydrocarbon chain packing. This is also manifested in the increase in permeability with the rise in *m* value. This probably also enables these vesicles to undergo facile fusion relative to their low ($m = 3$, 4) or high ($m = 20–22$) *m* value counterparts. The membranes derived from the lipids with *m* values 20–22 are thermally more resistant to melting. One point that deserves special mention is the evidence of strong interdigitation with high *m* values as revealed by EPR studies. The membranes from the same set of lipids have also been shown by X-ray diffraction studies to adopt interdigitated monolayer–bilayer hybrid structures. This may be one way by which the bolaphilic lipids that occur in thermophilic bacteria allow the resulting organisms to thrive at elevated temperatures. Finally, a novel feature of cholesterol interaction with dimeric lipids has been identified, that is, even after its inclusion up to physiologically relevant concentrations (30 mol%) present in mammalian-cell membranes, the gel–liquid crystalline melting transition is not abolished. Since eukaryotic cells are rich in cholesterol, such an observation may suggest that at the cellular level this may be a plausible mechanism by which solid-to-fluid transitions could still be maintained.

Clearly the covalent connection of two *monomeric* lipids by a simple $-(CH_2)_m-$ chain brings about effects at the membrane level that are much more pronounced than one would expect from seemingly trivial structural modifications at the lipid-molecular level. These findings emphasize the continuing need for new designs of synthetic lipid structures to expand our understanding of their behavior upon membrane formation.

Experimental Section

Methods and materials: Descriptions of the general procedures and the analytical instruments used for various spectroscopic characterizations have been described previously.[10b] *n*-Hexadecyl bromide, 1,2-isopropylidene glycerol, 1,3-dibromopropane, 1,4-dibromobutane, 1,5-dibromopentane, 1,6-dibromohexane, 1,12-dibromododecane, carbon tetrabromide, triphenylphosphine, 1,6-diphenyl-1,3,5-hexatriene (DPH), and riboflavin were purchased from Aldrich. 1,16-Dibromohexadecane, 1,20-dibromoeicosane, and 1,22-dibromodocosane were synthesized from tetradecane-1,14-dioic acid, eicosanedioic acid, and docosanedioic acid, respectively, by the reduction of their respective ethyl esters with lithium aluminium hydride in dry THF followed by bromination with HBr/H_2SO_4 at 80 °C for 24 h. They were separated by chromatography over a silica gel (60–120 mesh) column with hexane as the eluent.

Synthesis: Synthesis of monomeric lipids and different precursors of the dimeric lipids are synthesized as follows. First, 1,2-isopropylidene glycerol (**3**) was protected with benzyl chloride in dry benzene under refluxing conditions to obtain the corresponding benzyl ether **4**, and the isopropylidiene group was then removed with aqueous HCl/MeOH at room temperature to obtain *dl*-α-*O*-benzylglycerol.[28]

***dl*-α,β-Di-*O*-hexadecyl-*O*-benzylglycerol (5)**: A mixture of *dl*-α-*O*-benzylglycerol (5.0 g, 27.4 mmol), 1-bromohexadecane (18.5 g, 60.4 mmol), and powdered potassium hydroxide (5.9 g, 104.2 mmol) in dry benzene (50 mL) was stirred and refluxed for 24 h. The cooled mixture was diluted with chloroform (50 mL) and washed with water, and the organic layer was dried over anhydrous $MgSO_4$. The solvent was removed under vacuo and the crude product was purified by column chromatography over a silica gel column with a mixture of hexane and ethyl acetate to afford a viscous oil (10.0 g, 58%). ^{1}H NMR ($CDCl_3$, 400 MHz) $\delta = 0.90$ (t, 6H, CH_3), 1.10 (br s, 52H, CH_2), 1.50–1.80 (m, 4H, CH_2), 3.40–3.75 (m, 9H, OCH_2, OCH), 4.55 (s, 2H, CH_2Ph), 7.31 (s, 5H, aromatic Hs).

***dl*-α,β-Di-*O*-hexadecylglycerol (6)**: A solution of **5** (10 g, 15.8 mol) in methanol (150 mL) was hydrogenated over 5% Pd/C (0.2 g) for 24 h at 46 psi pressure during which almost all the starting materials were converted to the alcohol. Methanol was removed from the reaction mixture, and the solid mass obtained was heated with EtOAc. To remove the catalyst, this solution was filtered and kept at room temperature for crystallization. Upon repeated crystallizations, a flaky white solid was obtained (8 g, 92%), which was found to be pure by TLC ($R_f \approx 0.3$, $CHCl_3$). M.p. 47 °C (lit.[28] 48–49 °C); ^{1}H NMR ($CDCl_3$, 400 MHz) $\delta = 0.89$ (t, 6H, CH_3), 1.15–1.40 (br m, 52H, CH_2), 1.50–1.80 (m, 4H, CH_2), 3.40–3.75 (m, 9H, OCH_2, OCH).

***dl*-α,β-Di-*O*-hexadecylglycerol bromohydrin (7)**: A solution of Ph_3P (1.44 g, 4.32 mmol) in dry CH_2Cl_2 was added dropwise over a period of 30 min to a well-stirred solution of **6** (2.0 g, 3.62 mmol) and CBr_4 (2.42 g, 7.3 mmol) in dry CH_2Cl_2 at 0 °C. The reaction mixture was stirred at room temperature for another 8 h till TLC showed the disappearance of the starting material. CH_2Cl_2 was removed under vacuum, and the residual mass was repeatedly extracted with hexane. The combined extracts were evaporated to dryness. It was purified by column chromatography over a silica gel column with 100:1 hexane/EtOAc. The fraction which was collected using 50:1 hexane/EtOAc gave a viscous liquid on removal of organic solvent. It solidified on standing (1.97 g, 90%). TLC single spot ($R_f \approx 0.3$, hexane); ^{1}H NMR ($CDCl_3$, 200 MHz) $\delta = 0.89$ (t, 6H, CH_3), 1.15–1.40 (br m, 52H, CH_2), 1.54–1.80 (m, 4H, CH_2), 3.33–3.50 (m, 9H, OCH_2, OCH & CH_2Br).

***dl*-[1,2-Di-*O*-hexadecyl-3-(dimethylamino)]propane (8)**: Compound **7**(1 g, 1.65 mmol) was dissolved in a 40% methanolic solution of Me_2NH (20 mL, 102 mmol) in a screw-top pressure tube. The tube was sealed, and its contents were heated with stirring at ≈90 °C for 36 h. The solvent was removed to afford a crude residue, which was then treated with $NaHCO_3$ (5%, 25 × 2 mL) and the resulting product was extracted several times with

0947-6539/99/0508-2344 $ 17.50+.50/0 *Chem. Eur. J.* **1999**, *5*, No. 8

$CHCl_3$ (25 × 4 mL). The organic layer was separated, washed with brine (10 mL), and passed through anhydrous K_2CO_3. The solvent was removed to give a waxy semi-solid (0.9 g, 95%) which was found to be pure by TLC ($R_f \approx 0.8$, $CHCl_3$/MeOH, 10:1). ^{1}H NMR ($CDCl_3$, 200 MHz) $\delta = 0.89$ (t, 6H, CH_3), 1.15–1.60 (br m, 52H, CH_2), 2.32 (s, 6H, $N(CH_3)_2$), 2.42–2.60 (m, 2H, CH_2N), 3.45–3.75 (m, 7H, OCH_2, OCH).

***dl*-*N*-(1,2-Di-*O*-hexadecyl-3-propyl)-*N*,*N*,*N*-trimethylammonium bromide (1)**: Compound **7** (0.3 g, 0.5 mmol) was dissolved in a 30% ethanolic solution of NMe_3 (20 mL, 102 mmol)in a screw-top pressure tube. The tube was sealed, and its contents were heated with stirring at ≈90 °C for 36 h. The solvent was removed to afford a crude white mass, which was recrystallized several times from acetone/EtOAc (20:1) (0.3 g, 90%). It was found to be pure by TLC ($R_f \approx 0.5$, $CHCl_3$/MeOH, 10:1). M.p. 113–114 °C (lit.[29] 115–116 °C); ^{1}H NMR ($CDCl_3$, 400 MHz) $\delta = 0.89$ (t, 6H, CH_3), 1.20–1.40 (br m, 52H, CH_2), 1.60–1.80 (m, 4H, CH_2), 3.40–3.75 (s and m, 16H, $^+N(CH_3)_3$, OCH_2, OCH), 4.10–4.20 (m, 2H, N^+CH_2); $C_{38}H_{80}NO_2Br$ (662.97): calcd C 68.85, H 12.16, N 2.11; found C 68.63, H 11.97, N 1.87.

General procedure for the synthesis of bis(quaternary ammonium) lipids (2a–2h): A solution of *dl*-[1,2-*O*-hexadecyl-3-(dimethylamino)]propane **8** (1.0 mmol) and an appropriate α,ω-dibromoalkane (0.35 mmol) in dry EtOH was refluxed over a period of 48–72 h. It was cooled and the solvent was evaporated to give a crude solid. It was repeatedly washed with dry acetone to remove any traces of unreacted starting materials and finally subjected to repeated crystallizations from a mixture of acetone and methanol (≈9:1). This gave a white solid and the yields ranged from 60–75%. The purities of these lipids could be ascertained from TLC, the R_f ranged from ≈0.25 to ≈0.3 in 10:1 $CHCl_3$/MeOH. All compounds **2a–2h**, gave satisfactory ^{1}H NMR and IR spectra, and C,H,N analysis. Pertinent spectroscopic and analytical data are given below.

Propanediyl-α,ω-bis[*dl*-*N*-(1,2-di-*O*-hexadecyl-3-propyl)-*N*,*N*-dimethylammonium bromide] (2a): M.p. 175–178 °C; ^{1}H NMR ($CDCl_3$, 400 MHz) $\delta = 0.85$ (t, 12H, CH_3), 1.25–1.50 (br m, 104H, CH_2), 1.55–1.80 (br m, 8H, alkyl chain CH_2), 2.80–2.90 (br m, 2H, $N^+CH_2CH_2CH_2N^+$), 3.30–4.20 (m, 34H, $N^+(CH_3)_2$, OCH_2, OCH, $CH_2N^+CH_2$); $C_{77}H_{160}N_2O_4Br_2$ (1337.94): calcd C 69.12, H 12.05, N 2.09; found C 68.96, H 12.09, N 1.83.

Butanediyl-α,ω-bis[*dl*-*N*-(1,2-di-*O*-hexadecyl-3-propyl)-*N*,*N*-dimethylammonium bromide] (2b): M.p. 175–182 °C; ^{1}H NMR ($CDCl_3$, 400 MHz) $\delta = 0.85$ (t, 12H, CH_3), 1.25–1.50 (br m, 104H, $CH_2 \times 52$), 1.55–1.80 (m, 8H, alkyl chain CH_2), 2.19–2.30 (m, 4H, spacer chain CH_2), 3.20 (s, 12H, $N^+(CH_3)_2$), 3.30–3.52 (m, 8H, OCH_2), 3.60–4.20 (m, 14H, $CH_2N^+CH_2$, alkyl chain OCH_2, OCH); $C_{78}H_{162}N_2O_4Br_2$ (1351.97): calcd C 69.3, H 12.07, N 2.05; found C 69.58, H 12.36, N 1.99.

Pentanediyl-α,ω-bis[*dl*-*N*-(1,2-di-*O*-hexadecyl-3-propyl)-*N*,*N*-dimethylammonium bromide] (2c): M.p. 80 °C (soften), 88 °C (clear melt); ^{1}H NMR ($CDCl_3$, 400 MHz) $\delta = 0.85$ (t, 12H, CH_3), 1.25–1.40 (br m, 106H, CH_2, spacer chain $N^+CH_2CH_2CH_2$), 1.55–1.80 (m, 8H, alkyl chain CH_2), 2.15–2.19 (m, 4H, spacer chain $N^+CH_2CH_2$), 3.30–3.50 (m, 20H, $N^+(CH_3)_2$, alkyl chain OCH_2), 3.58–3.62 (m, 4H, OCH_2), 3.65–3.67 (m, 2H, OCH), 3.70–4.10 (m, 8H, $CH_2N^+CH_2$); $C_{79}H_{164}N_2O_4Br_2$ (1366.0): calcd C 69.46, H 12.1, N 2.05; found C 69.68, H 12.17, N 1.85.

Hexanediyl-α,ω-bis[*dl*-*N*-(1,2-di-*O*-hexadecyl-3-propyl)-*N*,*N*-dimethylammonium bromide] (2d): M.p. 78 °C (soften), 84 °C (clear melt); ^{1}H NMR ($CDCl_3$, 400 MHz) $\delta = 0.85$ (t, 12H, CH_3), 1.25–1.40 (br m, 108H, CH_2, spacer chain CH_2), 1.55–1.70 (m, 8H, alkyl chain CH_2), 2.10–2.19 (br m, 4H, spacer chain $N^+CH_2CH_2$), 3.30–3.50 (m, 20H, $N^+(CH_3)_2$, alkyl chain OCH_2), 3.55–3.57 (br m, 6H, OCH_2, OCH), 3.60–4.05 (m, 8H, $CH_2N^+CH_2$); $C_{80}H_{166}N_2O_4Br_2$ (1380.02): calcd C 69.63, H 12.12, N 2.03; found C 69.72, H 12.19, N 1.86.

Dodecanediyl-α,ω-bis[*dl*-*N*-(1,2-di-*O*-hexadecyl-3-propyl)-*N*,*N*-dimethylammonium bromide] (2e): M.p. 80 °C (soften), 95 °C (clear melt); ^{1}H NMR ($CDCl_3$, 400 MHz) $\delta = 0.85$ (t, 12H, CH_3), 1.25–1.50 (br m, 120H, CH_2, spacer chain CH_2), 1.55–1.70 (m, 8H, alkyl chain CH_2), 1.78–1.84 (m, 4H, spacer chain $N^+CH_2CH_2$), 3.30–3.50 (m, 20H, $N^+(CH_3)_2$, alkyl chain OCH_2), 3.58–3.59 (br m, 4H, OCH_2), 3.60–4.08 (m, 10H, $CH_2^+NCH_2$, OCH); $C_{86}H_{178}N_2O_4Br_2$ (1464.18): calcd C 70.55, H 12.25, N 1.91; found C 70.53, H 12.48, N 1.75.

Hexadecanediyl-α,ω-bis[*dl*-*N*-(1,2-di-*O*-hexadecyl-3-propyl)-*N*,*N*-dimethylammonium bromide] (2f): M.p. 65–70 °C; ^{1}H NMR ($CDCl_3$, 400 MHz) $\delta = 0.88$ (t, 12H, CH_3), 1.25–1.50 (s and br m, 128H, CH_2, spacer chain CH_2), 1.50–1.80 (m, 12H, alkyl chain CH_2, spacer chain $N^+CH_2CH_2$), 3.38–3.50 (m, 20H, $N^+(CH_3)_2$, alkyl chain OCH_2), 3.58 (apparent d, 4H, OCH_2), 3.60–4.30 (several m, 10H, $CH_2^+NCH_2$, OCH); $C_{90}H_{186}N_2O_4Br_2$ (1520.29): calcd C 71.10, H 12.33, N 1.84; found C 71.37, H 12.23, N 1.70.

Eicosanediyl-α,ω-bis[*dl*-*N*-(1,2-di-*O*-hexadecyl-3-propyl)-*N*,*N*-dimethylammonium bromide] (2g): M.p. 55–60 °C; ^{1}H NMR ($CDCl_3$, 400 MHz) $\delta = 0.88$ (t, 12H, CH_3), 1.25–1.40 (s and br m, 136H, CH_2, spacer chain CH_2), 1.50–1.80 (m, 12H, alkyl chain CH_2, spacer chain $N^+CH_2CH_2$), 3.36–3.50 (m, 20H, $N^+(CH_3)_2$, alkyl chain OCH_2), 3.52–3.61 (m, 4H, OCH_2), 3.62–4.10 (several m, 10H, $CH_2^+NCH_2$, OCH); $C_{94}H_{194}N_2O_4Br_2$ (1576.4): calcd C 71.62, H 12.40, N 1.78; found C 71.76, H 12.42, N 1.52.

Docosanediyl-α,ω-bis[*dl*-*N*-(1,2-di-*O*-hexadecyl-3-propyl)-*N*,*N*-dimethylammonium bromide] (2 h): M.p. 52–55 °C; ^{1}H NMR ($CDCl_3$, 400 MHz) $\delta = 0.88$ (t, 12H, CH_3), 1.25–1.40 (s and br m, 140H, CH_2, spacer chain CH_2), 1.50–1.80 (m, 12H, alkyl chain CH_2, spacer chain $N^+CH_2CH_2$), 3.40–3.44 (m, 20H, $N^+(CH_3)_2$, alkyl chain OCH_2), 3.57–3.58 (m, 4H, OCH_2), 3.62–4.10 (several m, 10H, $CH_2^+NCH_2$, OCH); $C_{96}H_{198}N_2O_4Br_2$ (1604.45): calcd C 71.87, H 12.44, N 1.75; found C 71.97, H 12.36, N 1.52.

Vesicle preparation

Method A: Dry films of a given lipid (2.5 mmol) film were obtained on the walls of Wheaton vials upon removal of chloroform from the solutions of the lipid in the same solvent. The requisite amount of water was added to this, and the resulting mixture was first kept at 4 °C for approximately 12 h and then vortexed to allow optimal hydration of the lipid film. It was vortexed for a few minutes and thawed to 70–75 °C for 10 min and then frozen with liquid N_2 for 15 min. These cycles were repeated three times to ensure optimal hydration. However, films of **2g** and **2h** did not form stable suspensions even after 5–7 freeze–thaw cycles. For effective dispersal these were sonicated with a bath sonicator (Sidilu Ultrasonic Bath) for 20 min at 80 °C and then subjected to freeze–thaw cycles. All the lipid suspensions including that of **2g** and **2h** were found to be stable for several days.

Method B: Solid lipid (2.5 mmol) was dissolved in $CHCl_3$ (5 mL) and to this an equal volume of pure water was added. The resulting two-phase mixture was briefly dispersed in a bath-sonicator (35 kHz) for 15 min at ambient temperature to produce an emulsion. From this, $CHCl_3$ was slowly removed under reduced pressure with a rotary evaporator. The resulting preparation was then subjected to 5–6 freeze–thaw cycles followed by a brief sonication for 5 min above 70 °C. This afforded stable translucent suspensions. Vesicles prepared by this protocol remained practically stable for several days as judged by the examination of the onset of turbidity of these suspensions as a function of time.

Transmission electron microscopy (TEM): This experiment used vesicles(2.5 mM) in water. Uranyl acetate (0.5% *w*/*v*) was used as the staining agent. Vesicles were prepared by the method B described above. One drop of a given vesicular solution was placed on a 400 mesh carbon–formvar™-coated copper grid. A JEOL-TEM 200CX electron microscope was used as described.[10k] The micrographs were recorded at magnifications of 70000 and 96000.

Dye entrapment and permeability: The vesicles from each of the above lipids (1 mg 1 mL^{-1}) were prepared by the method A in aqueous media containing riboflavin (20 μM) at pH 5.8. At ambient temperature 3 mL of a vesicle solution was loaded into a pre-equilibrated column (26 cm × 1 cm) of sephadex G-50M (Pharmacia). Upon elution with water (pH ≈5.8), gel-filtered fractions containing dye-loaded vesicles were pooled. An aliquot of a gel-filtered vesicle (1 mL) was placed into a cuvette and the pH was adjusted from 5.8 to ≈10.2 by the addition of KOH solution(66 μL, 0.03 M). Immediately upon mixing, time-dependent changes in the fluorescence emission at 514 nm (upon excitation at 374 nm) were measured at 25 ± 0.5 °C with a Hitachi Model F-4500 Spectrofluorimeter. The time-courses followed an apparent monoexponential decay, from which the rate constants were obtained by analyzing the data by means of a pseudo-first-order equation.

Calorimetry: Thermograms were recorded at two different lipid concentrations with a Perkin–Elmer DSC-4 instrument and an MC-2 ultrasensitive differential scanning calorimeter (Microcal) interfaced to a IBM compatible computer. Lipid dispersions at ≈120 mmol concentration were prepared by vortexing followed by freeze–thaw treatments. These were transferred into a steel pan (sample) which was sealed and kept at ≈90 °C inside the calorimeter to ensure optimal hydration. DSC heating and

cooling runs were recorded with the sample against a reference pan containing an identical volume of pure water at a scanning rate of 5 K min^{-1} in the Perkin–Elmer DSC-4 instrument. Samples (2.5 mM) for microcalorimetry made by the hydration of dry lipid film followed by sonication were degassed under vacuum prior to loading into the sample cell. The scan rate was 90 °C h^{-1}. A baseline recorded with pure water in both the sample and reference cells and normalized to mcal deg^{-1}, was subtracted from each heat capacity to eliminate any variations due to mismatch between the two cells. Excess heat capacity data for the transitions were filtered digitally and the normalized curves were established by connecting the baseline before and after the transition and then performing a point-by-point subtraction from this straight line. Transition enthalpies were calculated by numerical integration of the resulting heat capacity values as a function of temperature, [Eq. (1)]. Main transition entropies ΔS, in units of cal mol^{-1} K^{-1}, were estimated based on the assumption that at the T_m the two phases are at equilibrium, in which case Equation (2) applies, where ΔH_{cal} is expressed in cal mol^{-1} and T_m in Kelvin. The van't Hoff enthalpy ΔH_{vH} was obtained from the Equation (3) in which $\Delta T_{1/2}$ is the width at the half-maximum excess specific heat. These enthalpies were used to determine the cooperative unit (*CU*) of the transition, that is, the number of monomers undergoing the phase transition from the relationship expressed in Equation (4).

$$\Delta H_{cal} = \int Cp dT \quad (1)$$

$$\Delta S = \Delta H_{cal}/T_m \quad (2)$$

$$\Delta H_{vH} = 6.9\, T_m^2/\Delta T_{1/2} \quad (3)$$

$$CU = \Delta H_{vH}/\Delta H_{cal} \quad (4)$$

Fluorescence anisotropy studies: Upon excitation of 1,6-diphenyl-1,3,5-hexatriene (DPH) at 360 nm embedded in various vesicular solutions (2.5 mM), the fluorescence anisotropies (*r*) were measured with a Hitachi Model F4500 spectrofluorimeter. At each temperature, the emission spectra (390–480 nm) were recorded by adjusting the polarizers in four different positions. The anisotropy (*r*) at different temperatures for each vesicular solution was calculated by employing Perrin's equation, [Eq. (5)],

$$r = (I_\parallel - I_\perp G)/(I_\parallel + 2 I_\perp G) \quad (5)$$

in which $I_\parallel$ and $I_\perp$ are the observed intensities measured with polarizers parallel and perpendicular to the vertically polarized exciting beam, respectively. *G* is a factor used to correct for the inability of the instrument to transmit differently polarized light equally. For each aggregate, *r* versus *T* plots gave the information about the gel-to-liquid-crystalline phase change as a function of temperature. The values reported herein for *r* are the average values of three independent measurements. The systemic gel-to-liquid-crystalline phase transition temperatures were calculated from the midpoints of the breaks related to the temperature-dependent anisotropy values.

Dynamic light scattering (DLS): Light scattering measurements were measured at 25 °C on filtered vesicular solutions (Millex units, Pore size: 0.25 μm). Vesicles (1 mM) were prepared under identical conditions for all the lipids [bath sonication (Julabo USR3) for 10 min, at 70 °C and at 35 KHz]. A submicron particle-size analyzer employed an incident Kr^+ laser beam (647 nm) keeping the detector angle at 90°. An interfaced autocorrelator was used to generate the full autocorrelation of the scattered intensity. The time-correlated function was analyzed by a method of cumulants and the calculations imposed virtually unimodal distribution of particle size populations.

X-Ray diffraction and molecular modeling studies: X-ray diffraction and molecular modeling studies were carried out as described previously.[10a]

Electron paramagnetic resonance studies

Sample preparation: The spin probes, doxylstearic acids with the nitroxide group, that is, 5-(4,4-dimethyl-3-oxazolidinyl)oxyoctadecanoic acid, 5NS; 12-(4,4-dimethyl-3-oxazolidinyl)oxyoctadecanoic acid, 12NS, and 16-(4,4-dimethyl-3-oxazolidinyl)oxyoctadecanoic acid, 16NS were purchased from Sigma. Lipid dispersions were prepared by mixing the lipids with 1 mol% of the spin label probe in CH_2Cl_2 solution, evaporating off the solvent with a stream of dry nitrogen and then placing them under vacuum overnight. The dried lipids were then dispersed in water to a final concentration of 4 mg 0.4 mL^{-1} by hydrating for approximately 30 min followed by vortex mixing for 10 min at a temperature above the gel-to-fluid phase transition. The suspensions were transferred to 1 mm (i.d.), 100 μL glass capillaries, sealed at one end. The other end was sealed with parafilm. The sealed sample capillary tube was accommodated in a standard 4 mm quartz EPR tube.

EPR measurements: EPR spectra were measured on a Varian E-series spectrometer operating at a X-band frequency of 9.05 GHz. Conventional absorption EPR spectra were recorded at a modulation frequency of 100 kHz and a modulation amplitude of 4 G peak-to-peak, at a microwave power of 2 mW. The motional parameter, τ_0, can be derived from spectral parameters as described,[30] and is given by Equation (6), in which $K = 6.5 \times 10^{-10}$ s and is fixed arbitrarily at its limiting value in the case of rapid isotropic tumbling, W_0 is the width of the center line, and h_0 and h_{-1} are the heights of the center and high-field first-derivative lines respectively.

$$\tau_0 = K W_0 [(h_0/h_{-1})^{1/2} - 1] \quad (6)$$

The order parameter *S* gives a measure of the amplitude of motion of the long molecular axis about which the average orientation of the hydrocarbon chains occur in the lipid bilayers. It is obtained from the anisotropic outer and inner hyperfine splittings, $T_\parallel$ and $T_\perp$, respectively, by using the Equation (7), where T_{zz} and T_{xx} are the principal ^{14}N-hyperfine coupling tensors for a rigid lattice obtained from the single crystal spectra: $T_{zz} =$ 32.9 G, $T_{xx} = 5.9$ G. The maximum value of *S* is 1.0 for perfect order, while complete disorder results in a value of $S = 0$.

$$S = (T_\parallel - T_\perp)/(T_{zz} - T_{xx}) \quad (7)$$

Fusion assay

Liposome preparation: 1,2-Dioleoyl-*sn*-glycero-3-phosphoethanolamine-*N*-(7-nitro-1,3-benzoxadiazol-4-yl) (*N*-NBD-PE) and L-α-phosphatidylethanolamine-*N*-(lissamine rhodamine B sulfonyl) (Egg; *N*-Rh-PE) were purchased from Avanti Polar Lipids. Lipid films were dried under high vacuum and suspended at a concentration of 10 mg mL^{-1} in HEPES buffer (10 mM, pH 6.0). Lipids were dispersed by sonication with a bath sonicator for 5 min at ≈60 °C followed by one freeze–thaw treatment.

Fusion measurements: Vesicle fusion was monitored by resonance energy transfer (RET) fusion assay as described by Struck et al.[18] Vesicles were formed both with and without 0.6 mol% each of *N*-NBD-PE and *N*-Rh-PE and suspended at the concentration of 10 mg mL^{-1} in buffer. Labeled and unlabeled vesicles were mixed at a 1:1 ratio and diluted to a final lipid concentration of 50 μM in the above buffer. Fluorescence measurements were performed at 28 °C with a Hitachi F-4500 spectrofluorimeter at an excitation and emission wavelength of 475 and 580 nm, respectively. Fusion was initiated by the addition of 10 μL Na_2SO_4 solution (final concentration in the cuvette was 10 mM). The extent of fusion was determined by subjecting a one-to-one mixture of labeled and unlabeled vesicles to three cycles of freeze–thawing. This treatment has been shown[20] to be adequate for obtaining complete lipid mixing. Fused vesicles were diluted to 50 μM, and the fluorescence level of this suspension was set to 100% (F_{min}). The time course for each lipid mixing was normalized by subtracting the initial fluorescence (F_0) and dividing by the fluorescence achieved by infinite probe dilution (F_{min}). The percentage change in fluorescence was calculated as shown in Equation (8).

$$\%\Delta F/\Delta F_{min} = 100(F_0 - F)/(F_0 - F_{min}) \quad (8)$$

^{1}H NMR spectrsocopy

Vesicle preparation: $CHCl_3$ solutions of biscationic lipids with or without cholesterol were evaporated to dryness. The resulting lipid films were then hydrated in D_2O for ≈1 h at room temperature, vortexed thoroughly, and subjected to several freeze–thaw cycles (above the T_m value of the

0947-6539/99/0508-2346 $ 17.50+.50/0 *Chem. Eur. J.* **1999**, *5*, No. 8

corresponding lipid) keeping the vial protected from extraneous moisture during the preparation. The stable MLVs thus produced were rapidly transferred into NMR tubes and immediately closed under dry N_2.

Measurements: ^{1}H NMR spectra for each of these suspensions were recorded at 500 MHz on a Bruker DRX-500 Fourier transform Spectrometer equipped with a silicon graphics work station. The chemical shift due to the HDO peak was taken as the internal standard. The typical spectral conditions were as follows: pulse width 6.0 μs (flip angle 90°), sweep width 6009.62 Hz, data points 16 K, acquisition time 1.363 s, FID resolution of 0.3668 Hz/point, and the number of scans 270. ^{1}H NMR experiments were carried out with vesicular mixtures of **1**, **2a**, and **2g** containing 10, 20, and 30 mol % cholesterol. For comparison, ^{1}H NMR spectra were also recorded in the absence of cholesterol for each of the lipid vesicles. For each experiment, the lipid concentration was maintained at a constant 10 mM. NMR spectra were recorded above the T_m of the vesicular systems.

Acknowledgments

This work was supported by the Swarnajayanti Fellowship grant of the Department of Science and Technology. We are grateful to SERC for giving access to the computational facilities.

[1] a) K. M. Merz, Jr., B. Roux, *Biological Membranes. A Molecular Perspective from Computation and Experiment*, Birkhäuser, Boston, **1996**; b) J. L. Slater, C.-H. Huang, in *The Structure of Biological Membranes*, (Ed.: P. Yeagle), CRC, Boca Raton, FL, **1992**, pp. 175–210; c) D. Marsh, *CRC Handbook of Lipid Bilayers*, CRC, Boca Raton, FL, **1990**.

[2] a) J. B. F. N. Engberts, D. Hoekstra, *Biochim. Biophys. Acta* **1995**, *1241*, 323; b) O. Murillo, S. Watanabe, A. Nakano, G. W. Gokel, *Biochim. Biophys. Acta* **1995**, *117*, 7665; c) T. Kunitake, *Angew. Chem.* **1992**, *104*, 692; *Angew. Chem. Int. Ed. Engl.* **1992**, *31*, 709; d) H. Ringsdorf, B. Schlarb, J. Venzmer, *Angew. Chem.* **1988**, *100*, 117; *Angew. Chem. Int. Ed. Engl.* **1988**, *27*, 113; e) J. H. Fendler, *Science* **1984**, *223*, 888.

[3] a) N. A. J. M. Sommerdijk, T. H. L. Hoeks, M. Synak, M. C. Feiters, R. J. M. Nolte, B. Zwanenburg, *J. Am. Chem. Soc.* **1997**, *119*, 4338; b) S. J. Vigmond, T. Dewa, S. L. Regen, *J. Am. Chem. Soc.* **1995**, *117*, 7838; c) P. Klotz, L. A. Cuccia, N. Mohamed, G. Just, R. B. Lennox, *J. Chem. Soc. Chem. Commun.* **1994**, 2043; d) J. A. Killian, M. C. Koorengevel, J. A. Bouwstra, G. Gooris, W. Dowhan, B. de Kruijff, *Biochim. Biophys. Acta* **1994**, *1189*, 225.

[4] a) W. Hübner, H. H. Mantsch, M. Kates, *Biochim. Biophys. Acta* **1991**, *1066*, 166; b) S. M. Grunner, M. K. Jain, *Biochim. Biophys. Acta* **1985**, *818*, 352; Other examples of dimeric lipids are also known, see for example: M. DeRosa, A. Gambacorta, *Prog. Lipid Res.* **1988**, *27*, 153.

[5] a) *Molecular Mechanisms of Membrane Fusion*, (Eds.: S. Okhi, D. Doyle, T. D. Flanagan, S. W. Hui, E. Mayhew), Plenum, New York, **1988**; b) T. Ohnishi, T. Ito, *Biochemistry* **1974**, *13*, 881.

[6] O. Lockhoff, *Angew. Chem.* **1991**, *103*, 1639; *Angew. Chem. Int. Ed. Engl.* **1991**, *30*, 1611, and references therein.

[7] a) F. M. Menger, C. A. Littau, *J. Am. Chem. Soc.* **1991**, *113*, 1451; b) R. Zana, Y. Talmon, *Nature* **1993**, *362*, 228.

[8] a) S. De, V. K. Aswal, P. S. Goyal, S. Bhattacharya, *J. Phys. Chem.* **1996**, *100*, 11664; b) S. De, V. K. Aswal, P. S. Goyal, S. Bhattacharya, *J. Phys. Chem. B* **1997**, *101*, 5639; c) S. De, V. K. Aswal, P. S. Goyal, S. Bhattacharya, *J. Phys. Chem. B* **1998**, *102*, 6152.

[9] a) R. Oda, I. Huc, S. J. Candau, *Chem. Commun.* **1997**, 2105; b) F. L. Duivenvoorde, M. C. Feiters, S. J. van der Gaast, J. B. F. N. Engberts, *Langmuir* **1997**, *13*, 3737; c) R. Zana, *Curr. Opin. Colloid Interface Sci.* **1996**, *1*, 566; d) M. J. Rosen, *CHEMTECH* **1993**, 30.

[10] a) S. Bhattacharya, S. De, M. Subramanian, *J. Org. Chem.* **1998**, *63*, 7640; b) S. Bhattacharya, K. Snehalatha, S. K. George, *J. Org. Chem.* **1998**, *63*, 27; c) S. Bhattacharya, K. Snehalatha, *Langmuir* **1997**, *13*, 378; d) S. Bhattacharya, K. Snehalatha, *J. Org. Chem.* **1997**, *62*, 2198; e) S. Bhattacharya, S. S. Mandal, *Biochim. Biophys. Acta* **1997**, *1323*, 29; f) S. Bhattacharya, S. Haldar, *Biochim. Biophys. Acta* **1996**, *1283*, 21; g) S. Bhattacharya, S. De, *Chem. Commun.* **1996**, 1283; h) S. Ghosh, K. R. K. Easwaran, S. Bhattacharya, *Tetrahedron Lett.* **1996**, *37*, 5769; i) S. Bhattacharya, K. Snehalatha, *Langmuir* **1995**, *11*, 4653; j) S. Bhattacharya, S. Haldar, *Langmuir* **1995**, *11*, 4748; k) S. Bhattacharya, S. De, *J. Chem. Soc. Chem. Commun.* **1995**, 651.

[11] a) S. Bhattacharya, S. S. Mandal, *Biochemistry* **1998**, *37*, 7764; b) J.-P. Vigneron, N. Oudrhiri, M. Fauquet, L. Vergely, J.-C. Bradley, M. Basseville, P. Lehn, J.-M. Lehn, *Proc. Natl. Acad. Sci. USA* **1996**, *93*, 9682.

[12] In a preliminary communication, we described some properties of these dimeric lipids, see: S. Bhattacharya, S. De, S. K. George, *Chem. Commun.* **1997**, 2287.

[13] a) J. M. Delfino, S. L. Schreiber, F. M. Richards, *J. Am. Chem. Soc.* **1993**, *115*, 3458. b) D. H. Thompson, K. F. Wong, R. Humphry-Baker, J. J. Wheeler, J.-M. Kim, S. B. Rananavare, *J. Am. Chem. Soc.* **1992**, *114*, 9035; c) R. A. Moss, J.-M. Li, *J. Am. Chem. Soc.* **1992**, *114*, 9227; d) E. A. Runquist, G. M. Helmkamp, Jr., *Biochim. Biophys. Acta* **1988**, *940*, 10; e) J.-M. Kim, D. H. Thompson, *Langmuir* **1992**, *8*, 637.

[14] a) T. Kunitake, Y. Okahata, S. Yasunami, *Chem. Lett.* **1981**, 1397; b) H. Fukuda, K. Kawata, H. Okuda, S. L. Regen, *J. Am. Chem. Soc.* **1990**, *112*, 1635.

[15] a) S. Karaborni, K. Esselink, P. A. J. Hilbers, B. Smit, J. Karthauser, N. M. van Os, R. Zana, *Science* **1994**, *266*, 254; b) D. Damino, Y. Talmon, R. Zana, *Langmuir* **1995**, *11*, 1448.

[16] a) R. Bartucci, T. Pali, D. Marsh, *Biochemistry* **1993**, *32*, 274; b) J. M. Boggs, J. T. Mason, *Biochim. Biophys. Acta* **1986**, *863*, 231.

[17] J. M. Boggs, G. Rangaraj, *Biochim. Biophys. Acta* **1985**, *816*, 221.

[18] D. K. Struck, D. Hoekstra, R. E. Pagano, *Biochemistry* **1981**, *20*, 4093.

[19] N. Düzgüneş, T. M. Allen, J. Fedor, D. Papahadjopoulos, *Biochemistry* **1987**, *26*, 8435.

[20] A. Relini, D. Cassinadri, Q. Fan, A. Gulik, Z. Mirghani, M. De Rosa, A. Gliozzi, *Biophys. J.* **1996**, *71*, 1789.

[21] M. G. L. Elferink, J. van Breemen, W. N. Konings, A. J. M. Driessen, J. Wilschut, *Chem. Phys. Lipids* **1997**, *88*, 37.

[22] K. Block, in *Biochemistry of Lipids and Membranes*, (Eds.: D. E. Vance, J. E. Vance), The Benzamin/Cummins, Menlo Park, CA, **1985**, pp. 1–24.

[23] a) P. L. Yeagle, *Biochim. Biophys. Acta* **1985**, *822*, 267; b) W. K. Subczynski, A. Wisniewska, J.-J. Yin, J. S. Hyde, A. Kusumi, *Biochemistry* **1994**, *33*, 7670.

[24] a) R. B. Gennis, in *Biochemistry: Molecular Structures and Functions*, Springer, New York, **1989**, chapter 8; b) M. B. Sankaran, T. E. Thompson, *Biochemistry* **1990**, *29*, 10676.

[25] M. C. Block, L. L. M. van Deenen, J. de Gier, *Biochim. Biophys. Acta* **1977**, *464*, 509.

[26] N. Chatterjee, H. Brockerhoff, *Biochim. Biophys. Acta* **1978**, *511*, 116.

[27] a) P. Almeida, W. Vaz, T. E. Thompson, *Biochemistry* **1992**, *31*, 6739; b) M. B. Sankaran, T. E. Thompson, *Proc. Natl. Acad. Sci. USA* **1991**, *88*, 8686; c) C. Mateo, A. Reyes, A. U. Acuna, J.-C. Bronchon, *Biophys. J.* **1995**, *68*, 978; d) S. Scarlata, *Biophys. Chem.* **1997**, *69*, 9.

[28] M. Kates, T. H. Chan, N. Z. Stanacev, *Biochemistry* **1963**, *2*, 394.

[29] R. A. Moss, S. Ganguli, Y. Okumura, T. Fujita, *J. Am. Chem. Soc.* **1990**, *112*, 6391.

[30] a) J. M. Boggs, M. A. Moscarello, *J. Membrane Biol.* **1978**, *39*, 75; b) S. Eletr, A. D. Keith, *Proc. Natl. Acad. Sci. USA* **1972**, *69*, 1353; c) J. Seelig, *J. Am. Chem. Soc.* **1970**, *92*, 3881.

Received: November 3, 1998 [F1424]